

Ablation Induced by Single- and Multiple-Femtosecond Laser Pulses in Lithium Niobate

H. Chen, X. Chen*, Y. Zhang, and Y. Xia

Department of Physics, State Key Laboratory on Fiberoptic Local Area Communications Networks and Advanced Optical Communications Systems, Shanghai Jiao Tong University, Shanghai, 200240 China

*e-mail: xfchen@sjtu.edu.cn

Received May 25, 2007

Abstract—We present results on the surface-damage threshold of lithium niobate after single- and multiple-femtosecond laser pulse irradiation at the pulse duration of 80 fs, with a 800-nm wavelength, and a repetition rate of 1 kHz. The surface-ablation threshold was found to decrease significantly with an increase in the pulse number applied to the surface until reaching an almost constant level due to an incubation effect, which is attributed to the laser-induced defect formation. The threshold of lithium niobate under a single shot is found to be 2.82 J/cm^2 , and the threshold fluence for an infinite number of pulses $F_{\text{th}}(\infty)$ converges to a common value of $0.52 \pm 0.06 \text{ J/cm}^2$ for $N > 80$. The results have the potential for application in laser micromachining and the fabrication of related optical devices and applications in frequency conversion by a femtosecond laser in lithium niobate.

PACS numbers: 42.65.Re; 77.84.Dy

DOI: 10.1134/S1054660X07120079

1. INTRODUCTION

Damage and micromachining in dielectrics irradiated under femtosecond lasers have been intensively studied. An extremely localized treatment of materials can often not be achieved by using long laser pulses, since thermal diffusion in the material and, moreover, the interaction of the laser light with the ablation plasma may dominate and prevent high-quality processing. In contrast to light irradiation with nano- and picosecond pulses [1, 2], the main advantages of femtosecond lasers, such as the direct writing of structures, higher processing speeds, and minimal contamination of processed material, make them an attractive tool for precision writing in the fields of micro- and nanotechnology. For these advantages, femtosecond laser-assisted modifications are being extensively used in different optical materials, such as polymers [3], optical glass [4–6] and sapphire [7, 8]. In addition, the laser ablation of highly reflective materials, e.g., metals [9], and semiconductors [10], has also been investigated.

Lithium niobate is one of the most used crystalline dielectric materials at present, which is referred as “silicon in nonlinear optics,” because it has excellent acoustooptic, electrooptic, nonlinear optical, and optical waveguiding properties. Furthermore, LiNbO_3 is a well-known nonlinear crystal with a high refractive index of 2.2 and a large transparent range of 0.4–5.0 μm , making it an ideal candidate material for photonic crystals. Because of these unique advantages, the femtosecond laser modification in LiNbO_3 has also attracted increasing attention in recent years [11–17].

The behavior of modification by the femtosecond laser depends strongly on the material’s properties and the parameters of the laser. If the laser fluence applied to the sample exceeds a certain fluence F_{th} (the material’s fluence threshold), ablation occurs. In this paper, we discuss the shot-number dependency in the surface-damage threshold of lithium niobate for femtosecond-laser pulse. The surface-ablation threshold was found to decrease significantly with an increase in the pulse number applied to the surface until reaching an almost constant level due to an incubation effect, which is attributed to a laser-induced defect formation.

2. EXPERIMENT SETUP

The laser used in the experiments was an amplified Ti:sapphire laser system, whose standard output is 80 fs, 0.9 mJ, and 800 nm at 1-kHz repetition rate. The energy of the pulse can be changed continuously with the combination of a half-wave plate and a polarizer. The linearly polarized Gaussian laser beam was focused vertically onto the front surface of the sample using a 50-mm-focal-length lens. A Gaussian spatial beam profile with a radius ($1/e^2$) of $\sim 30 \mu\text{m}$ at the spot was achieved. The sample was moved using a two-dimensional stepping-motor-controlled stage to make each pump pulse irradiate on a fresh area. Furthermore, a desired pulse train can be obtained by controlling a shutter. The sample of crystal LiNbO_3 used in this study is $20 \times 10 \text{ mm}^2$ in diameter, 1-mm thick, and polished on both sides. After ablation, the sample was cleaned by the ultrasonic. The Ti:sapphire femtosecond laser setup used for processing is shown in Fig. 1.

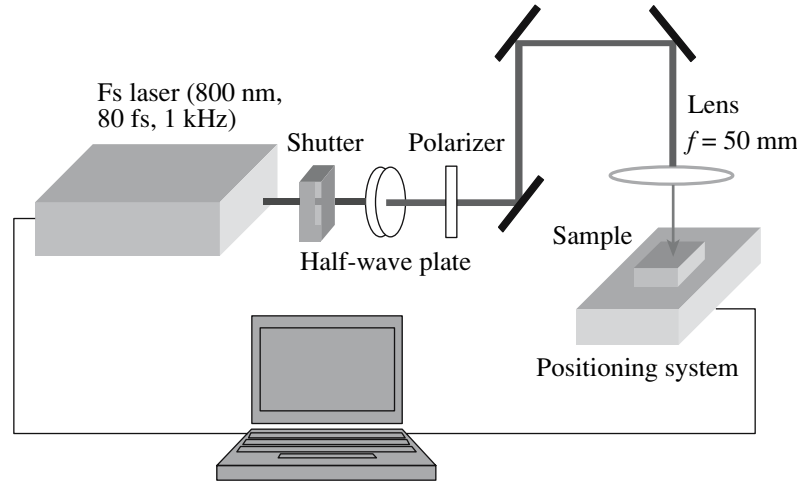


Fig. 1. Experimental setup of the femtosecond-laser micromachining.

3. RESULTS AND DISCUSSION

In general, the laser ablation is material specific and depends strongly on several parameters, such as laser wavelength, spatial-beam profile, beam-focus position relative to the sample surface, laser fluence, pulse duration, and the number of laser shots. For the ablation threshold investigations, we generated a dot matrix of laser-induced modifications on the sample surface by varying the number of shots and the laser energy. We assume that ablation takes place only in the central area of the laser beam, when the radial fluence distribution $F(r) = F_0 \exp(-2r^2/\omega_0^2)$ exceeds the ablation-threshold fluence F_{th} . Where ω_0 is the Gaussian beam radius, F_0 is the maximum laser fluence, which depends linearly on the incident-laser pulse energy E_{pulse} , and can be written as $F_0 = 2E_{pulse}/\pi\omega_0^2$ [18]. Supposing the diameter of the ablated area is D , the laser threshold is, then, $F(r = D/2) = F_{th}$. Thus, we can obtain the relation between the diameter of the damaged area and the maximum laser fluence F_0 [19]:

$$D^2 = 2\omega_0^2 \ln\left(\frac{F_0}{F_{th}}\right). \quad (1)$$

If we obtain a series of D under different pulse energies, thus we can obtain the beam radius and the laser-ablation threshold. In our experiment, the measurement of the diameters D of the laser-damaged areas was completed with an optical microscope. Some typical snapshot images of the ablated area under single- and multiple-femtosecond laser pulses are given in Fig. 2. A typical image of the ablated area under a single-shot experiment, which was taken from a 400 \times microscope, is shown in Fig. 2a. In this case, the peak intensity of the pulse was 7.08 J/cm². Figures 2b and 2c show the ablated area of the sample under 20 and 100 fs laser

pulses at an energy density of 6.37 and 7.78 J/cm², respectively. The micrograph of a typical array written by different pulse numbers and energies is shown in Fig. 2d, which was taken from a 100 \times microscope.

The shape of the ablated area is not perfectly round; this may be due to the fact that the incident pulse was not ideally a Gaussian-profile shape and the sample itself is anisotropic [11].

As mentioned earlier, the laser-ablation threshold can be obtained by getting a series of D under different pulse energies. Figure 3 shows the measured fluence dependence of the squared diameter of the ablated area

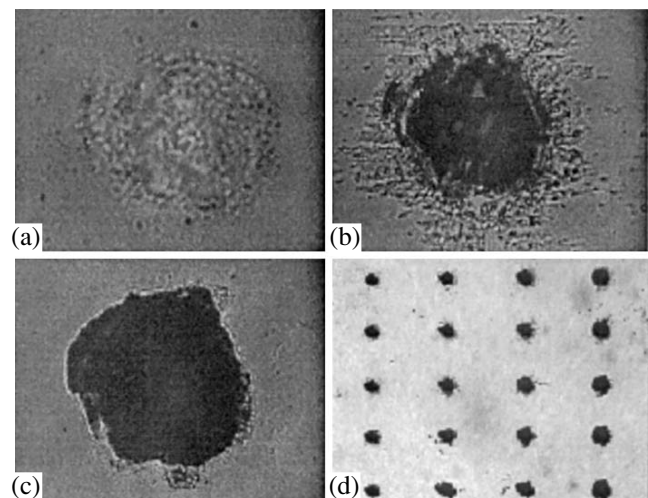


Fig. 2. (a) The micrograph of an ablated spot of the LN surface under a single shot; (b) the micrograph of an ablated spot of the LN surface under 20 shots; (c) the micrograph of an ablated spot of the LN surface under 100 shots; (d) the ablation matrix, where the shot numbers increase from top to bottom and the power increases from left to right.

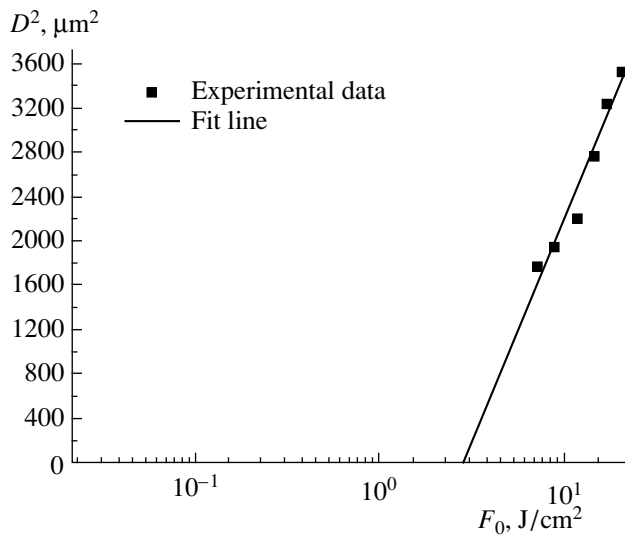


Fig. 3. The relation between the squared diameters D^2 of the ablated areas and the applied laser fluence for single-pulse processing of lithium niobate in air: $\tau = 80$ fs, $\lambda = 800$ nm.

with a single shot. According to Eq. (1), the slope of the fitted line gives some information regarding the beam radius of the input pulse and we can obtain $\omega_0 \approx 29$ μm . By extrapolating the fitted line to $D^2 = 0$, the threshold is found to be $F_{\text{th}} = 2.82$ J/cm^2 .

Figure 4 shows the ablated results for squared diameters versus the applied laser fluence for multishot experiments. The modification threshold F_{th} can be estimated by extrapolating the linear fit to $D^2 = 0$. Thus, the ablation thresholds are 1.01, 0.87, 0.68, and 0.56 J/cm^2 for 20, 60, 80, and 100 pulses, respectively, for lithium niobate in air.

It can be clearly seen that the threshold fluence is influenced by the number of shots impinging on the crystal surface. This so-called incubation effect appears due to the accumulation of laser-induced material defects that are precursors to the surface damage. As discussed in several previous studies [8, 20], the incubation effect saturates exponentially with the number of shots N , which can be described by

$$F_{\text{th}}(N) = F_{\text{th}}(\infty) + [F_{\text{th}}(1) - F_{\text{th}}(\infty)] \exp(-k(N-1)), \quad (2)$$

where $F_{\text{th}}(\infty)$ is the threshold fluence for an infinite number of pulses, $F_{\text{th}}(1)$ is the threshold fluence for a single shot, and k is the incubation parameter that characterizes the strength of the defect accumulation and the increase in the photon absorption [20]. We investigated the role of incubation in LiNbO_3 by determining the threshold fluences $F_{\text{th}}(N)$ for different numbers of shots N between 1 and 1000 at the wavelength 800 nm. The results obtained at $\lambda = 800$ nm are shown in Fig. 5, where the line represents the best fit of Eq. (2) to the experimental data.

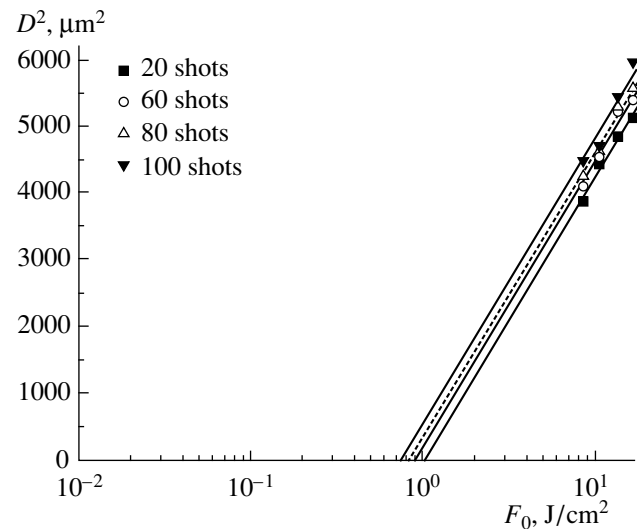


Fig. 4. The relation between the squared diameters D^2 of the ablated areas and the applied laser fluence for multiple-pulse processing of lithium niobate in air: $\tau = 80$ fs, $\lambda = 800$ nm.

The surface-ablation threshold was found to decrease significantly with an increase in the pulse number applied to the surface until reaching an almost constant level due to an incubation effect, which is attributed to a laser-induced defect formation [20]. The threshold fluence for an infinite number of pulses $F_{\text{th}}(\infty)$ converged to a common value of 0.52 ± 0.06 J/cm^2 for $N > 80$ and incubation parameter k , which has an average value of 0.06.

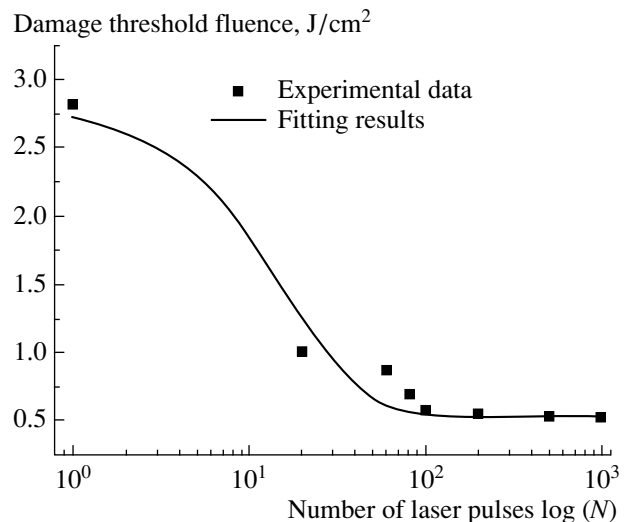


Fig. 5. Threshold fluence as a function of the number of pulses N at $\lambda = 800$ nm, $\tau = 80$ fs. The threshold fluence for an infinite number of pulses $F_{\text{th}}(\infty)$ converges to a common value of 0.52 ± 0.06 J/cm^2 for $N > 80$.

4. CONCLUSIONS

In conclusion, surface ablation experiments with Ti:sapphire laser pulses on lithium niobate were demonstrated at the pulse duration of 80 fs, with an 800-nm wavelength, and a repetition rate of 1 kHz. We measured the damage thresholds of lithium niobate under different numbers of pulses. The surface-ablation threshold was found to decrease significantly with an increase in the pulse number applied to the surface until reaching an almost constant level due to an incubation effect. It was found that the threshold of lithium niobate under a single shot is about 2.82 J/cm^2 , and the threshold fluence for an infinite number of pulses $F_{\text{th}}(\infty)$ converged to a common value of $0.52 \pm 0.06 \text{ J/cm}^2$ for $N > 80$ and the incubation parameter k , which has an average value of 0.06. The results have potential application in laser micromachining and in the fabrication of related optical devices and applications in frequency conversion by a femtosecond laser in lithium niobate.

ACKNOWLEDGMENTS

This research was supported by the National Natural Science Foundation of China (nos. 60477016 and 10574092), and the National Basic Research Program "973" of China (2006CB806000).

REFERENCES

1. B. N. Chichkov, C. Momma, S. Nolte, et al., *Appl. Phys. A* **63**, 109 (1996).
2. M. S. Amer, M. A. El-Ashry, L. R. Dosser, et al., *Appl. Surf. Sci.* **242**, 162 (2005).
3. S. Küper and M. Stuke, *Appl. Phys. Lett.* **54**, 4 (1989).
4. B. C. Stuart, M. D. Feit, S. Herman, et al., *J. Opt. Soc. Am.* **813**, 459 (1996).
5. B. C. Stuart, M. D. Feit, S. Herman, et al., *Phys. Rev. B* **53**, 1749 (1996).
6. J. Ihlemann, B. Wolff, and P. Simon, *Appl. Phys. A* **54**, 363 (1992).
7. Xiaoxi Li, Tianqin Jia, Donghai Feng, and Zhizhan Xu, *Appl. Surf. Sci.* **225**, 339 (2004).
8. X. C. Wang, G. C. Lim, H. Y. Zheng, et al., *Appl. Surf. Sci.* **228**, 221 (2004).
9. P. T. Mannion, J. Magee, E. Coyne, et al., *Appl. Surf. Sci.* **223**, 275 (2004).
10. I. Zergioti and M. Stuke, *Appl. Phys. A* **67**, 391 (1998).
11. Guangyong Zhou and Min Gu, *Phys. Lett. A* **87**, 241 107 (2005).
12. R. R. Thomson, S. Campbell, I. J. Blewett, et al., *Appl. Phys. Lett.* **88**, 111 109 (2006).
13. A. H. Nejadmalayeri and P.R. Herman, *Opt. Lett.* **31**, 2987 (2006).
14. J. Burghoff, H. Hartung, S. Nolte, and A. Tünnermann, *Appl. Phys. A* **86**, 165 (2007).
15. J. Burghoff, C. Grebing, S. Nolte, and A. Tünnermann, *Appl. Phys. Lett.* **89**, 081 108 (2006).
16. A. Ródenas, J. A. Sanz García, D. Jaquea, et al., *J. Appl. Phys.* **100**, 033521 (2006).
17. D. C. Deshpande, A. P. Malshe, E. A. Stach, et al., *J. Appl. Phys.* **97**, 074316 (2005).
18. J. Bonse, J. M. Wrobel, J. Krüger, and W. Kautek, *Appl. Phys. A* **72**, 89 (2001).
19. J. Güdde, J. Hohlfeld, J. G. Müller, and E. Mattias, *Appl. Surf. Sci.* **40**, 127 (1998).
20. D. Ashkenasi, M. Lorenz, R. Stoian, and A. Rosenfeld, *Appl. Surf. Sci.* **150**, 101 (1999).